Journal of Experimental Botany, Vol. 57, No. 15, pp. 4215–4224, 2006
doi:10.1093/jxb/erl198 Advance Access publication 3 November, 2006

Journal of Experimental Botany

RESEARCH PAPER

A permeation–diffusion–reaction model of gas transport in cellular tissue of plant materials

Q. Tri Ho[1,*], Bert E. Verlinden[1], Pieter Verboven[1], Stefan Vandewalle[2] and Bart M. Nicolaï[1]

[1] *BIOSYST-MeBioS, Faculty of Bioscience Engineering, Katholieke Universiteit Leuven, Willem de Croylaan 42, B-3001 Leuven, Belgium*

[2] *Scientific Computing Research Group, Computer Science Department, Katholieke Universiteit Leuven, Celestijnenlaan 200A, B-3001 Leuven, Belgium*

Received 18 May 2006; Accepted 12 September 2006

Abstract

Gas transport in fruit tissue is governed by both diffusion and permeation. The latter phenomenon is caused by overall pressure gradients which may develop due to the large difference in O_2 and CO_2 diffusivity during controlled atmosphere storage of the fruit. A measurement set-up for tissue permeation based on unsteady-state gas exchange was developed. The gas permeability of pear tissue was determined based on an analytical gas transport model. The overall gas transport in pear tissue samples was validated using a finite element model describing simultaneous O_2, CO_2, and N_2 gas transport, taking into account O_2 consumption and CO_2 production due to respiration. The results showed that the model described the experimentally determined permeability of N_2 very well. The average experimentally determined values for permeation of skin, cortex samples, and the vascular bundle samples were $(2.17\pm1.71)\times10^{-19}$ m^2, $(2.35\pm1.96)\times10^{-19}$ m^2, and $(4.51\pm3.12)\times10^{-17}$ m^2, respectively. The permeation–diffusion–reaction model can be applied to study gas transport in intact pears in relation to product quality.

Key words: Controlled atmosphere, diffusion, gas transport, measurement set-up, modelling, permeation, storage, *Pyrus communis*.

Introduction

Gas exchange plays a fundamental role in biological plant materials. Gas transport is caused by differences in gas composition between the applied external atmosphere and the internal atmosphere due to O_2 consumption and CO_2 production during respiration and fermentation (Kader, 1988). In fruit tissue, the gas-filled intercellular spaces are thought to be the main pathways for gas transport through plant organs needed for respiration. Several methods have been developed to measure the gas transport properties of various horticultural commodities (Cameron and Yang, 1982; Banks, 1985) for which it was assumed that the skin was the only barrier to gas diffusion and the fruit internal gas concentration was constant. This assumption does not hold for all types of commodities, especially not for fruit with a high tissue density (Banks and Kays, 1988; Lammertyn *et al*., 2003*a*). Due to barriers between the ambient atmosphere and the cells, where respiration takes place, considerable gas gradients between the external and internal atmospheres may occur (Rajapakse *et al*., 1990; Lammertyn *et al*., 2003*a*). Some controlled atmosphere storage disorders such as core breakdown in pear have been related to limited gas transport inside the fruit (Lammertyn *et al*., 2003*a*, *b*).

Gas transport in fruit and other bulky storage organs have macroscopically been described with Fick's laws of diffusion, assuming an effective diffusion process which is driven by concentration gradients (Burg and Burg, 1965; Cameron and Yang, 1982; Banks, 1985). During gas exchange, O_2 in the gas phase diffuses through the skin of the fruit followed by diffusion in the intercellular system of pore spaces. Subsequently, O_2 exchange between the intercellular atmosphere and the cellular solution occurs through the cell membrane. Finally, the O_2 diffuses within the cytoplasm to the point of O_2 consumption. Respiratory CO_2 follows the reverse path. The rate of gas movement

* To whom correspondence should be addressed. E-mail: quangtri.ho@biw.kuleuven.be

depends on the properties of the gas molecules and the physical properties of the intervening barriers (Kader, 1988; Nobel, 1991). Development of the theory that connects the microscopic to the macroscopic description of mass transport in biological materials has been subjected to several investigations (Wood and Whitaker, 1998; Wood *et al*., 2002; Quintard *et al*., 2006). In these studies, the transport on the microscale was volume-averaged to a macroscopic equation containing *effective parameters* for the macroscopic properties of the biological materials. Recently, a macroscopic reaction–diffusion model for the macroscopic level that incorporates both gas diffusion and respiration was found appropriate for calculating the gas transport inside the fruit (Mannapperuma *et al*., 1991; Lammertyn *et al*., 2003*a*, *b*). Effective diffusion properties of the fruit were determined by measuring the concentration of gas exchange between two chambers of a measurement set-up separated by a tissue slice (Lammertyn *et al*., 2001; Schotsmans *et al*., 200, 2004; Ho *et al*., 2006*a*). The results showed that the CO_2 diffusivity of the tissue was much higher than O_2 diffusivity. It was hypothesized that CO_2 is not only transported in the gas phase but also in the water phase from cell to cell, due to its high solubility in the solution, while O_2 is mainly transported in the gas phase of the gas-filled intercellular spaces. If the CO_2 diffusivity is higher than that of O_2, the produced CO_2 leaves the fruit at higher rates than O_2 is entering the fruit. This would lead to a pressure difference between the internal parts of the fruit and the external atmosphere. Therefore, besides gas diffusion driven by concentration gradients, gas transport in the fruit occurs by permeation due to total pressure gradients in the fruit tissues.

Gas permeation can be defined as the transport process in a porous medium in which the gas flow is described by Darcy's law (Geankoplis, 1993; Bird *et al*., 2002). In fruit tissue, the intercellular space existing within a highly complicated network of gaseous channels can be considered as such a porous medium. Several authors have studied the gas diffusion properties of fruit tissue; however, gas permeation in fruit has only received attention in early work of the 1960s (Marcellin, 1974) A further complication caused by small pressure gradients is the flow of N_2 which may contribute on the alleviation of this gradient. Pressure changes inside packages filled with horticultural produce, due to O_2, CO_2, and N_2 transport in relation to package shrinkage, were described by Talasila and Cameron (1997). However, with the exception of the model of Schotsmans *et al*. (2003) for gas transport, no models reported in the literature include transport of N_2 in fruit tissue.

The objectives of this paper are (i) to determine gas permeation properties of pear tissue, (ii) to determine N_2 diffusivity in pear tissue, and (iii) to expand existing diffusion models for O_2 and CO_2 transport in fruit with N_2 and permeation transport.

Materials and methods

Materials

Pears (*Pyrus communis* L. cv. 'Conference') were harvested on 8 September 2004 at the preclimacteric stage at the Fruitteeltcentrum (Rillaar, Belgium), cooled, and stored according to commercial protocols for a period of 21 d at –0.5 °C preceding CA storage (2.5 kPa O_2, 0.7 kPa CO_2 at –0.5 °C) until they were used for the experiments.

Pear flesh samples were first cut with a professional slice cutter (EH 158-L, Graef, Germany), subsequently small cylinders with a diameter of 24 mm were cut with a cork borer. The thickness of the sample was measured with a digital caliper (Mitutoyo Ltd., UK, accuracy ± 0.01 mm) and ranged from 1–2 mm. For the skin samples, a razor blade was used to remove the flesh until a thickness of less than 1 mm was obtained. Cortex tissue samples were taken in the radial direction at the equatorial region of the pear and in the vertical axis, containing vascular bundles. Because a pear has an asymmetric shape, large gradients in gas concentration were not expected in the two tangential directions perpendicular to the radial direction inside the fruit. It is, therefore, not important to know the gas transport properties in these directions accurately. A schematic view of the sampling protocol is given in Fig. 1.

Model of gas transport in pear tissue

Flux of gas transport: A mass flux of a gas component $\mathbf{j}$ (mol m^{-2} s^{-1}) describing the diffusion and permeation processes through the pear tissue samples is given by

$$\mathbf{j} = C\mathbf{u} + \mathbf{j}_d \tag{1}$$

with C (mol m^{-3}) the concentration of gas, $\mathbf{u}$ (m s^{-1}) the apparent velocity vector, and $\mathbf{j}_d$ (mol m^{-2} s^{-1}) the flux of gas diffusion through a barrier of tissue. In equation (1), the first term of the right hand side is the mass flow carried in the bulk flow of the fluid due to permeation, while the second term results from a concentration gradient (Fick's law).

Permeation through the tissue by a pressure gradient can be described by Darcy's law for laminar flow in porous media (Bird *et al*., 2002).

$$\mathbf{u} = -\frac{K}{\mu}\nabla P \tag{2}$$

with K (m^2) the permeation coefficient, P (Pa) the pressure, μ (Pa s^{-1}) the viscosity of the gas, ∇ (m^{-1}) the gradient operator.

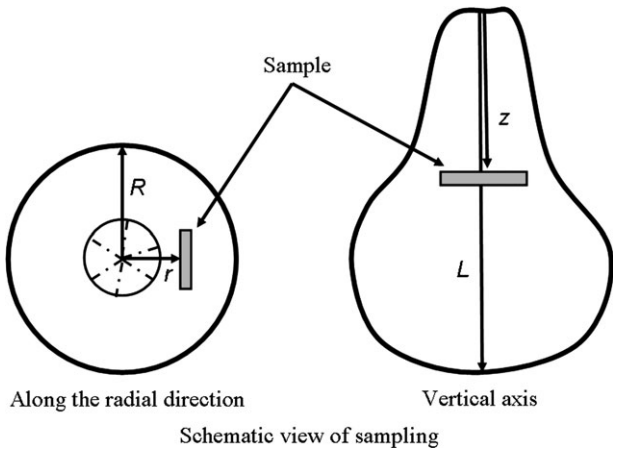

Fig. 1. Schematic view of sampling protocol.

For laminar flow in porous media such as tissue, permeation coefficients can be determined empirically and are usually considered to be independent of the gas passing the tissue.

The gas diffusion through the tissue can be approximated by Fick's first law of diffusion (Bird *et al*., 2002), which states that the flux of a gas diffusing through a barrier of tissue $\mathbf{j}_d$ is proportional to the concentration gradient over this barrier, ∇C (mol m^{-4}) with the effective diffusion coefficient D (m^2 s^{-1}) acting as a proportionality coefficient

$$\mathbf{j}_d = -D\nabla C \tag{3}$$

Representative elemental volume: The tissue structure of the fruit is a combination of cells, cell walls, and intercellular spaces. A representative elemental volume (*REV*) of the tissue is considered to contain two phases, namely the intracellular liquid phase of the cells and cell walls and the air-filled intercellular space (Fig. 2). The volume fraction of the intercellular space is assigned a value ε, the porosity of the tissue. Assuming local equilibrium at a certain concentration of the gas component i in the gas phase $C_{i,g}$ (mol m^{-3}), the concentration of the compound in the liquid phase of fruit tissue normally follows Henry's law. If the tissue has a porosity ε, the volume-averaged concentration $C_{i,tissue}$ (mol m^{-3}) of species i is then defined as:

$$C_{i,tissue} = \varepsilon C_{i,g} + (1-\varepsilon)RTH_i C_{i,g} \tag{4}$$

with H_i (mol m^{-3} kPa^{-1}) Henry's constant of component i (i is O_2, CO_2, or N_2), R the universal gas constant (8.314 J mol^{-1} K^{-1}), and T (K) the temperature.

From this definition, the following property of the tissue is derived

$$\alpha_i = \varepsilon + (1-\varepsilon)RTH_i = \frac{C_{i,tissue}}{C_{i,g}} \tag{5}$$

The parameter α_i is called the gas capacity of the component i in the tissue.

Gas transport equation in tissue: On the microscale, gas transport by diffusion and permeation in the intercellular spaces and diffusion and respiration in the cellular liquid phase were considered. Transport of gas i in those two phases is governed by the following equations

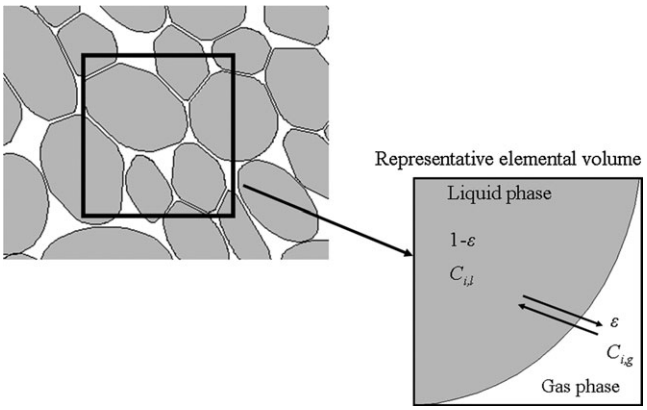

Fig. 2. A representative elemental volume of tissue. The symbol ε is the porosity of the tissue, $C_{i,g}$ (mol m^{-3}) and $C_{i,l}$ (mol m^{-3}) are the concentration of specie i in the gas and liquid phases, respectively.

$$\varepsilon\frac{\partial C_{i,g}}{\partial t} + \nabla(\varepsilon \mathbf{u}_g C_{i,g}) = \nabla(\varepsilon D_{i,g})\nabla C_{i,g} \tag{6}$$

$$(1-\varepsilon)\frac{\partial C_{i,l}}{\partial t} = \nabla\big((1-\varepsilon)D_{i,j}\big)\nabla C_{i,l} + (1-\varepsilon)R_{i,l} \tag{7}$$

with $C_{i,g}$ (mol m^{-3}) the concentration of i in the gas phase, $D_{i,g}$ (m^2 s^{-1}) the diffusion coefficient in the gas phase, $\mathbf{u}_g$ (m s^{-1}) the velocity vector in the gas phase of tissue, $C_{i,l}$ (mol m^{-3}) the concentration of i in the liquid phase, $D_{i,l}$ (m^2 s^{-1}) the diffusion coefficient in the liquid phase of tissue, $R_{i,l}$ (mol m^{-3} s^{-1}) the respiration rate (mol m^{-3} s^{-1}) and t (s) the time.

Since gas transfer in the intercellular spaces was considered to be in equilibrium with the liquid phase of the cells, the mass transport of component i in the liquid phase in equation (7) could be rewritten as

$$(1-\varepsilon)RTH_i\frac{\partial C_{i,g}}{\partial t} = \nabla\big((1-\varepsilon)(D_{i,l}RTH_i)\big)\nabla C_{i,g} + (1-\varepsilon)R_{i,l} \tag{8}$$

Adding equations (6) and (8) yields a single volume-averaged transport equation over the *REV*:

$$\begin{aligned}(\varepsilon + (1-\varepsilon)RTH_i)\frac{\partial C_{i,g}}{\partial t} + \nabla(\varepsilon \mathbf{u}_g C_{i,g}) \\ = \nabla(\varepsilon D_{i,g} + (1-\varepsilon)D_{i,l}RTH_i)\nabla C_{i,g} \\ + (1-\varepsilon)R_{i,l}\end{aligned} \tag{9}$$

Using the effective diffusivity D_i (m^2 s^{-1}), the effective permeation velocity vector $\mathbf{u}$ (m s^{-1}) and the effective respiration term R_i (mol m^{-3} s^{-1}) of the tissue, respectively, defined by

$$D_i = \varepsilon D_{i,g} + (1-\varepsilon)D_{i,j}RTH_i \tag{10}$$

$$\mathbf{u} = \varepsilon \mathbf{u}_g \tag{11}$$

$$R_i = (1-\varepsilon)R_{i,l} \tag{12}$$

one obtains

$$\alpha_i\frac{\partial C_{i,g}}{\partial t} + \nabla(\mathbf{u}C_{i,g}) = \nabla D_i \nabla C_{i,g} + R_i \tag{13}$$

with the boundary condition:

$$C_{i,b} = C_{i,\infty} \tag{14}$$

$C_{i,b}$ (mol m^{-3}) and $C_{i,\infty}$ (mol m^{-3}) are the concentration of gas i at the boundary surface of tissue and the external condition, respectively.

Permeation was described using Darcy's law (equation 2). The relation between the concentration C and pressure P can be expressed by using the ideal gas law $P{=}CRT$. Therefore, equation (2) can be rewritten as follows

$$\mathbf{u} = -\frac{KRT}{\mu}\nabla\big(\textstyle\sum C_{i,g}\big) \tag{15}$$

The estimation of permeation coefficient K and the effective diffusivity will be discussed in the next section. The respiration of tissue was described by Ho *et al*. (2006*a*).

Measurement of gas transport parameters

Measurement set-up: The system used to measure gas transport properties of fruit tissue consisted of two chambers (measurement chamber and flushing chamber) separated by a disc-shaped tissue sample (Fig. 3; Ho *et al*., 2006*a*). The chambers were metal

cylinders screwed together, holding a PVC ring containing a tissue sample glued on it with cyano-acrylate glue. A rubber O ring was used to seal the PVC ring between the two chambers and to ensure that all gas transport between the two chambers took place through the tissue sample. Two inlet and outlet gas channels were used to flush the gases in the measurement chamber and flushing chamber. Pressure sensors (PMP 4070, GE Druck, Germany, accuracy $\pm 0.04\%$) monitored the pressure changes in each chamber during the measurements. The temperature of the system was kept constant at 20.0 ± 0.5 °C by submerging the set-up in a temperature-controlled water bath (F10-HC, Julabo Labor Technik GmbH, Seelbach, Germany, accuracy ± 0.5 °C). The preparation of the samples was described by Ho *et al.* (2006*a*). The sealing of chambers was checked and validated before the experiments by rapidly changing the temperature of the water bath. When the pressure inside the measurement chamber increased correspondingly this indicated proper sealing.

Diffusion coefficients of O_2, CO_2, and N_2: Data of diffusion coefficients of respiratory gasses (O_2 and CO_2) were reported by Ho *et al.* (2006*b*), the diffusivity of N_2 was measured with the same set-up described by Ho *et al.* (2006*a*, *b*). Once the sample was attached to the diffusion cell, the measurement and the flushing chambers were flushed with, respectively, 70 kPa N_2, 30 kPa O_2, 95 kPa N_2, and 5 kPa O_2, at 10 l h^{-1}, humidified, and passed through a heat exchanger to prevent the sample from drying and cooling down while flushing the two chambers. After 30 min, the in- and outlet valves of the measurement chamber were closed, and the decrease in O_2 partial pressure and total pressure of the measurement chamber was monitored for 6 h. The O_2 concentration was measured in the measurement chamber with fluorescent optical probes (Foxy-Resp, Ocean Optics, Duiven, The Netherlands). The difference in total pressure between the two chambers was logged and was kept smaller than 1.5 kPa to minimize permeation. The (second) permeation term was correspondingly omitted in equation (13); the CO_2 production was negligible for this case. The N_2 concentration was determined indirectly from the total pressure and the O_2 concentration. D_{O_2} and D_{N_2} were estimated by fitting the solution of the transport equation (13) for O_2 and N_2 to the measured concentration profiles in the measurement chamber. Equation (13) was solved numerically according to the procedure described in Ho *et al.* (2006*a*). The CO_2 diffusivity was available from previous experiments (Ho *et al.*, 2006*b*). R_{O_2} was set to -2.47×10^{-4} mol m^{-3} s^{-1} (Ho *et al.*, 2006*a*).

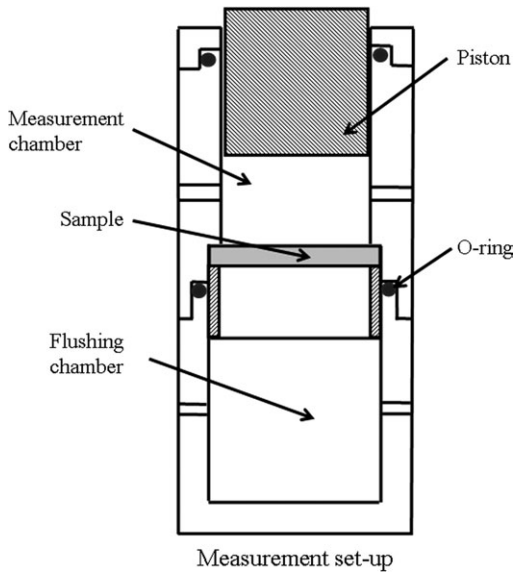

Fig. 3. Schematic of the measurement set-up for tissue diffusivity and permeability measurements. The set-up consists of two chambers (measurement chamber and flushing chamber) separated by a disc-shaped tissue sample. A gas partial pressure gradient is established by flushing the measurement and flushing chamber by different gas mixtures.

Permeation coefficient: In the permeation experiment, the measurement and the flushing chambers were flushed with nitrogen at 10 l h^{-1}, humidified, and passed through a heat exchanger to prevent the sample from drying and cooling down while flushing the two chambers. Nitrogen gas was used in the experiment as it has no physiological activity so that the source term R_{N_2} vanishes from equation (13). The pressure in the measurement set-up was adjusted to get a 6 kPa pressure difference between the measurement and flushing chambers. The total pressure difference between the two chambers was not higher than 7 kPa, to prevent mechanical deformation and even damage of the tissue which would falsify the results. Finally, the in- and outlet valves of the measurement chamber were closed, and the decrease in pressure of the measurement chamber was monitored for at least 4 h.

Because of the absence of O_2, there was no transport of this gas in the experiment. Similarly, based on some preliminary simulations it was found that the CO_2 production through fermentation was also negligible, so that transport of CO_2 could be omitted as well. For this particular measurement set-up, a lumped mass balance of a one component gas (N_2) in the measurement chamber could be used in one-dimensional form as follows:

$$V\frac{\partial C}{\partial t} + Aj = 0 \tag{16}$$

with V (m^3), the volume of the measurement chamber, A (m^2) the surface of the tissue area, t (s) time. Note that the vector quantities now become scalar quantities in one dimension. Substituting equation (1) into equation (16) yields

$$V\frac{\partial C}{\partial t} + Cu_x A = -Aj_d \tag{17}$$

with u_x (m s^{-1}) the apparent velocity of gas in the x-direction through the tissue sample based on the total cross-section of the sample. The x-direction was chosen perpendicular to the sample surface and pointing from the measurement to the flushing chamber. Clearly, C decreases when u_x is positive (permeation flow from the measurement chamber to the flushing chamber) and when the diffusive flux is negative.

The relation between the concentration C and pressure P can be found from the ideal gas law. Equation (3) can then be rewritten in one dimension as follows

$$j_d = -D\frac{\partial C}{\partial x} = -\frac{D}{RT}\frac{\partial P}{\partial x} \tag{18}$$

Permeation through the tissue by a pressure gradient can be deduced for one-dimensional laminar flow in porous media as follows

$$u_x = -\frac{K}{\mu}\frac{\partial P}{\partial x} \tag{19}$$

The gradient of total pressure can be approximated as the difference in total pressure between two chambers over a barrier which is the sample with a thickness L (m).

$$\frac{\partial P}{\partial X} = \frac{P_f - P(t)}{L} \quad (20)$$

with P_f (kPa), the constant pressure in the flushing chamber, and $P(t)$ (kPa) the pressure in the measurement chamber at the time t.

Substitution of equation (20) into equations (18) and (19), respectively, and substituting the results into equation (17) yields

$$\frac{V\partial P(t)}{\partial t} = \left(P_f - P(t)\right)\left(\frac{KA}{\mu L}P(t) + \frac{AD}{L}\right) \quad (21)$$

The analytical solution of equation (21) describing the pressure change in the measurement chamber $P(t)$ (kPa) with the time t (s) then is

$$P(t) = \frac{P_f + \frac{D\mu}{K}}{1 - \left(1 - \frac{P_f + \frac{D\mu}{K}}{P_0 + \frac{D\mu}{K}}\right)\exp\left(-\frac{AK}{VL\mu}\left(P_f + \frac{D\mu}{K}\right)t\right)} - \frac{D\mu}{K} \quad (22)$$

with P_o (kPa) the initial pressure in the measurement chamber.

The permeation K of the tissue was determined by fitting the experimental data to equation (22) by using an iterative least squares estimation procedure written in MATLAB (The Mathworks, Inc., Natick, USA).

Validation experiments

The aforementioned experiments were used to determine permeation properties of the pear tissue by using only N_2. However, air is a mixture of three main components: O_2, CO_2, and N_2 and the gas transport in the tissue is a combination of diffusion and permeation processes. Validation experiments were performed to verify whether the measured permeation properties could also be applied to O_2 and CO_2. In addition, a gas transport model was used to predict the effect of permeation on the estimation of diffusion coefficient.

For model validation purposes, an experiment was performed with gradients applied such that transport of O_2 and CO_2 took place in the opposite direction. This experimental validation was done based on the diffusion experiment described by Ho *et al.* (2006*a*). In validation experiment 1 (measurement chamber 30 kPa O_2, 0 kPa CO_2, and 70 kPa N_2; flushing chamber 5 kPa O_2, 30 kPa CO_2, and 65 kPa N_2) and 2 (measurement chamber 20 kPa O_2, 5 kPa CO_2, and 75 kPa N_2; flushing chamber 10 kPa O_2, 20 kPa CO_2, and 70 kPa N_2), the initial gas conditions were chosen such that there was pressure built-up in the measurement chamber. In validation experiment 3, gas conditions were such that the difference in total pressure between the two chambers remained smaller than 1.5 kPa and permeation was negligible (measurement chamber 30 kPa O_2, 3 kPa CO_2, and 67 kPa N_2; flushing chamber 5 kPa O_2, 8 kPa CO_2, and 87 kPa N_2).

Transport of O_2, CO_2, and N_2 was described by means of the convection diffusion model (equations 13 and 14) in which permeation through the barrier of tissue by the pressure gradient is described by Darcy's law (equation 15). The parameters of O_2 and CO_2 diffusion and respiration were described by Ho *et al.* (2006*a*). The porosity of the pear tissue was taken equal to 0.07 (Schotsmans *et al.*, 2004). R_{O_2} was set to -2.47×10^{-4} mol m^{-3} s^{-1} and R_{CO_2} was set equal to $-0.95R_{O_2}$ (Ho *et al.*, 2006*a*). The system (13) to (15) of transport equations was solved by means of the finite element method. The measurement chamber and the sample tissue were considered as two materials consisting of 20 1D linear elements each resulting in 41 nodes in total. The diffusion coefficient of the gas molecules in air at 20 °C was set equal to 6×10^{-5} m^2 s^{-1} (Lide, 1999). The discretization was carried out in the Femlab 3.1 package (Comsol AB, Stockholm, Sweden). More details can be found in Ho *et al.* (2006*a*).

Results

O_2 and N_2 diffusivities

In Fig. 4, the O_2 and total pressure profiles in the measurement chamber are shown as a function of time. The O_2 partial pressure decreased while the total pressure profiles were almost constant during the measurement. As there was no pressure built-up in the measurement chamber, permeation was negligible in this case; the permeation term in the left-hand side of equation (13) was therefore omitted. At the beginning of the experiment, a step decrease of the total pressure in the measurement chamber in Fig. 4 indicated that the in- and outlet valves of the measurement chamber were closed to stop flushing. In the measurement chamber the high O_2 partial pressure caused O_2 transport from the measurement to the flushing chamber while N_2 diffused in the opposite direction from the flushing chamber to the measurement chamber, which was at a lower N_2 partial pressure. The diffusivity of N_2 was estimated based on the total pressure profile and the O_2 partial pressure profile in the measurement chamber. In addition, the diffusivity of O_2 was also estimated and compared with N_2 diffusivity. The results are given in Table 1. The diffusivity of N_2 was more or less equal to the diffusivity of O_2 in the cortex tissue. A paired t test showed that there was no significant difference between the O_2 and N_2 diffusivity. Furthermore, a t test between groups of samples showed that the diffusivity of the skin was the smallest, and the diffusivity in the vertical axis was higher than the diffusivity along the radial direction.

Gas permeation properties

In Fig. 5, the pressure profile in the measurement chamber as a function of time is shown for a typical permeation experiment with pure N_2. The gas transport from the measurement chamber to the flushing chamber by permeation caused a pressure decrease during time. Figure 5 shows that the decrease of pressure for tissue samples along the vertical axis of the pear was faster compared with tissue samples along the radial direction. The model described the experimentally determined values very well. The resulting estimated permeation coefficients are shown in Table 1. The average values for the permeation coefficients of the skin, cortex tissue along the radial direction and vertical axis were $(2.17\pm1.71)\times10^{-19}$ m^2, $(2.35\pm1.96)\times10^{-19}$ m^2, and $(4.51\pm3.12)\times10^{-17}$ m^2, respectively (Table 1). A high variation was found for the estimated values. From a statistical analysis, the estimated permeation values of the skin and cortex tissue along the radial direction were not significantly different, while the permeation coefficient of tissue along the vertical axis was much higher compared with the permeation coefficient of cortex tissue along the radial direction. The temperature of

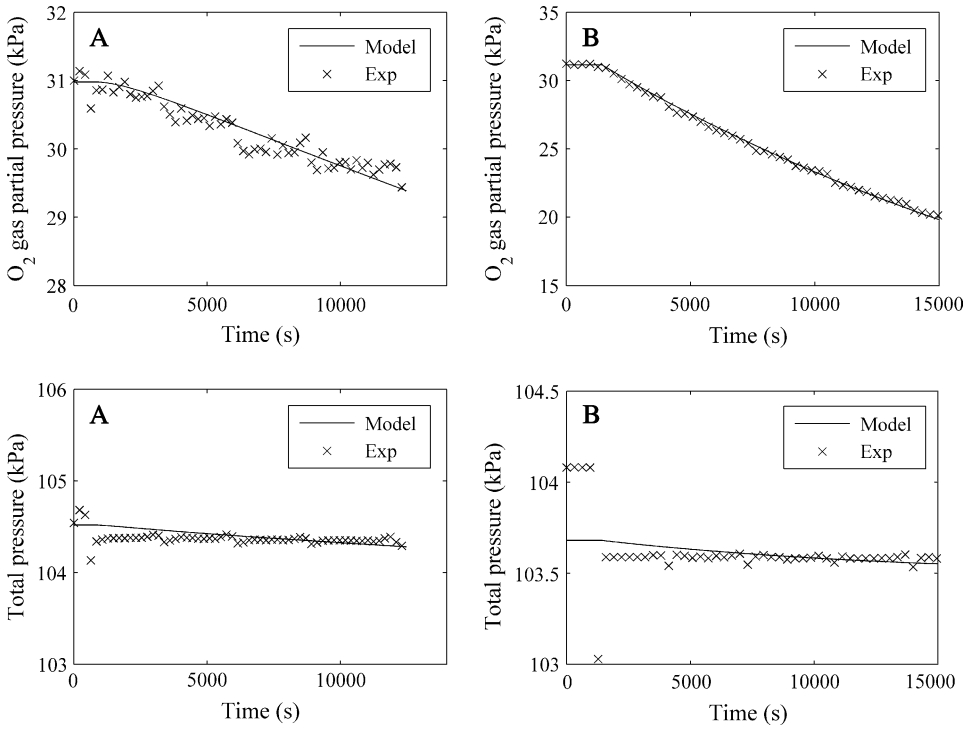

Fig. 4. Typical O_2 partial pressure (top) and total pressure (bottom) time profiles in the measurement chamber for diffusion of O_2 and N_2 through the pear cortex tissue (balanced pressure diffusion experiment, measurement chamber 70 kPa N_2, 30 kPa O_2 initially, flushing chamber 95 kPa N_2, 5 kPa O_2) in the radial direction (A) and along the vertical axis (B). The symbols and lines denote the measurements and model predictions [equations (13–14)], respectively. The permeation in equation (13) term was omitted here as the total pressure was almost constant during both experiments.

Table 1. *Estimated gas transport properties in the pear tissue*

	Skin		Cortex tissue along the radial direction		Cortex tissue along the vertical axis	
	Value[a]	#[b]	Value	#	Value	#
D_{O_2} (m^2 s^{-1})	$(0.100\pm0.034)\times10^{-9}$	8	$(0.28\pm0.15)\times10^{-9}$	6	$(1.11\pm0.71)\times10^{-9}$	7
D_{N_2} (m^2 s^{-1})	$(0.106\pm0.032)\times10^{-9}$	8	$(0.267\pm0.17)\times10^{-9}$	6	$(1.08\pm0.71)\times10^{-9}$	7
K (m^2)	$(2.17\pm1.71)\times10^{-19}$	8	$(2.35\pm1.96)\times10^{-19}$	7	$(4.51\pm3.12)\times10^{-17}$	16

[a] $\pm$ the standard deviation.
[b] # the number of samples.

the set-up was also important since the total pressure in the measurement chamber changed with temperature according to the ideal gas law. Small fluctuations of the experimental values are due the fluctuation of the temperature during the measurement. A change of 0.5 °C in temperature gave an effect of about 0.17 kPa on the total pressure in the measurement chamber.

Validation

In validation experiments 1 and 2, the initial gas conditions in the measurement chamber were chosen in such a way that large CO_2 concentration between the two chambers was created. Due to the larger diffusivity of CO_2 in cortex tissue compared with those of O_2 and N_2, a pressure rise was noticed during the measurement. Plots of the measurement data, the simulation of gas transport with permeation and without permeation are shown in Fig. 6. At the beginning of the experiment, a step decrease of the total pressure in the measurement chamber in Fig. 6 indicated that the in- and outlet valves of the measurement chamber were closed off from flushing. Validation showed that the model with permeation was more in agreement with the experiment compared with the diffusion only.

In validation experiment 3, the difference in total pressure between the two chambers was smaller than 1.5 kPa. A good agreement was found for both simulations between measurements and model predictions (Fig. 6). The effect of the permeation term in the equation on the gas transport was small in this experiment. The simulated profile of the O_2 partial pressure in the measurement

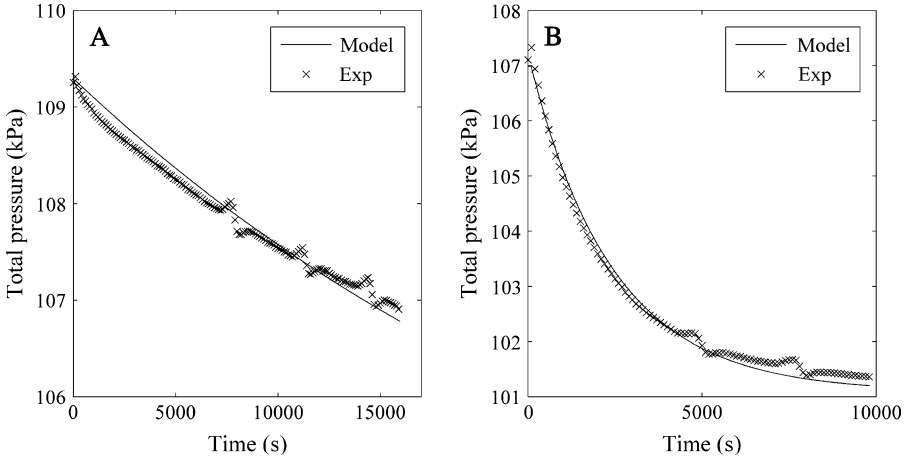

Fig. 5. Total pressure in the measurement chamber as a function of time (N_2 permeation experiment) for cortex tissue in the radial direction (A) and along the vertical axis (B). Symbols denote measurement and lines denote model predictions according to equation (22).

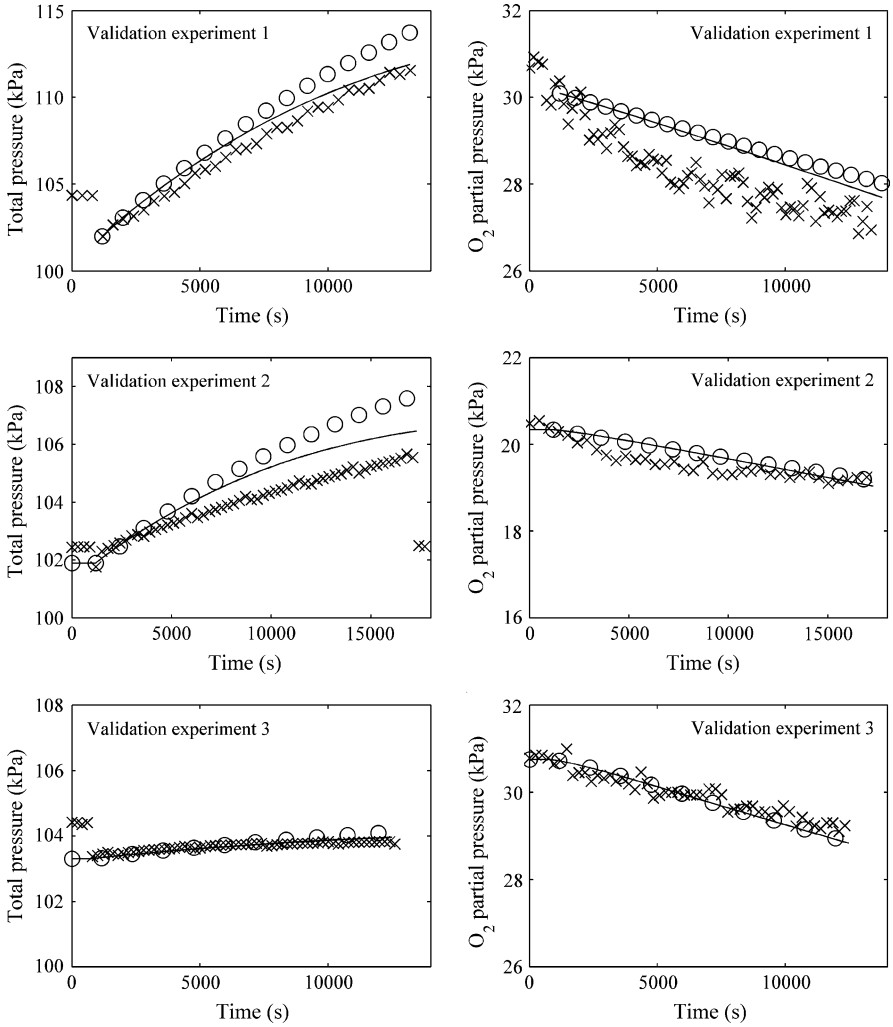

Fig. 6. Total pressure and O_2 partial pressure profiles in the measurement chamber as a function of time for a sample of cortex tissue. Symbol '×' indicates measured data, symbol 'o' indicates the gas transport model prediction with diffusion and without permeation. The solid line (—) indicates the gas transport model prediction with diffusion as well as permeation taken into account. In validation experiment 1 and 2, the conditions were chosen such as to produce a total pressure difference between both chambers: in validation experiment 3 the conditions caused only a negligible pressure difference.

chamber as a function of time in the diffusion model coincided with the diffusion model incorporating permeation. The permeation term in the left-hand side of the equation (13) is not important in this case and gas permeation can be considered negligible for estimating diffusion parameters.

The total pressure in the measurement chamber for the three validation experiments is shown in Fig. 7. Variability between replicate measurements due to biological variability is clearly visible. A good agreement was found between the models and experiments with different initial gas conditions.

Discussion

O_2 and N_2 diffusivity

The results show that there was no significant difference between O_2 and N_2 diffusivity. During the whole experiment the total pressure drop over the sample was constant and very small to non-existent (<0.5 kPa). Because the experiment was done for binary gas mixtures, the constant pressure in the measurement chamber implied that N_2 molecules diffuse at the same rate in the opposite direction to the O_2 molecular diffusion. Further, O_2 and N_2 have a comparable and low solubility in water. Therefore, gas exchange through the tissue for O_2 and N_2 probably happens through gas-filled intercellular space, where diffusion is the main mechanism.

The results obtained in this research for the diffusivity of O_2 of the skin, cortex tissue along the radial direction, and cortex tissue along the vertical direction were $(0.1\pm0.034)\times10^{-9}$ m^2 s^{-1}, $(0.28\pm0.15)\times10^{-9}$ m^2 s^{-1}, and $(1.11\pm0.71)\times10^{-9}$ m^2 s^{-1} while the diffusivity of N_2 of the skin, cortex tissue along the radial direction, and cortex tissue along the vertical direction were $(0.106\pm0.032)\times10^{-9}$ m^2 s^{-1}, $(0.267\pm0.17)\times10^{-9}$ m^2 s^{-1}, and $(1.08\pm0.71)\times10^{-9}$ m^2 s^{-1}. Measurement of the O_2 and CO_2 diffusivity by Ho *et al*. (2006*b*) showed that O_2 diffusivities in the skin, cortex tissue along the radial direction, and cortex tissue along the vertical direction was $(0.186\pm0.078)\times10^{-9}$ m^2 s^{-1}, $(0.222\pm0.037)\times10^{-9}$ m^2 s^{-1}, and $(1.11\pm0.72)\times10^{-9}$ m^2 s^{-1} while the CO_2 diffusivity in the skin, cortex tissue along the radial direction, and cortex tissue along the vertical direction was $(0.506\pm0.315)\times10^{-9}$ m^2 s^{-1}, $(2.32\pm0.21)\times10^{-9}$ m^2 s^{-1}, and $(6.97\pm3.79)\times10^{-9}$ m^2 s^{-1}. A good agreement was found between the O_2 diffusivity in the present experiment compared to the values reported by Ho *et al*. (2006*b*).

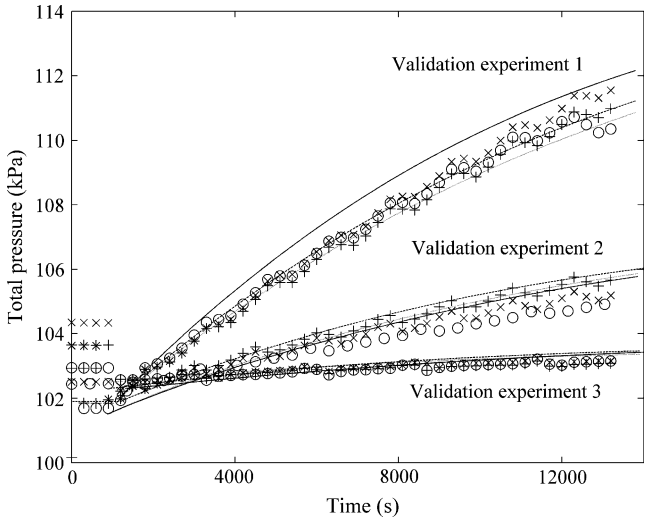

Fig. 7. Total pressure in the measurement chamber as a function of time for samples of cortex tissue. Lines indicate model predictions of the total pressure including permeation; symbols denote measured values (three replicate experiments). In validation experiments 1 and 2, the conditions were chosen such as to produce a total pressure difference between both chambers: in validation experiment 3 the conditions caused only a negligible pressure difference.

Schotsmans *et al*. (2003) found that the O_2 diffusivity of cortex and skin after 3 months of storage were $(0.33\pm0.24)\times10^{-9}$ m^2 s^{-1} and $(0.43\pm0.17)\times10^{-9}$ m^2 s^{-1}, respectively. In a more recent publication, the same authors (Schotsmans *et al*., 2004) found that O_2 diffusivity in the flesh of 'Jonica' (52.8×10^{-9} m^2 s^{-1}) and 'Braeburn' (16.2×10^{-9} m^2 s^{-1}) apples was much higher than that of pear flesh tissue. Zhang and Bunn (2000) also found similar O_2 diffusivity values ($18.1–19.0\times10^{-9}$ m^2 s^{-1}) for different apple cultivars. We believe that the differences in diffusivity in fruit cultivars can be attributed to differences in intercellular space volume. In this context, Schotsmans *et al*. (2004) showed that the intercellular space volume of cortex tissue of 'Jonica' and 'Braeburn' apples was 16% and 10% while it was only 5–7% for 'Conference' pear. Ongoing research concentrates on multiscale models to provide further evidence for this hypothesis.

A higher diffusivity in the vertical axis compared with the diffusivity along the radial direction was observed. While vascular bundles are filled with sap in intact plants, they may be not fully filled with sap during storage of the fruit as it typically loses water. It is, therefore, well possible that the vascular bundles along the axis of the pear indeed facilitate gas transport. Moreover, the orientation of the cells along the vertical axis could be different from that of cells in the radial direction, and further difference in gas transport properties may be due to enhanced interconnectivity of the gas intercellular space along the vertical axis compared with the radial direction. Sorz and Hietz (2006) also found that O_2 diffusion in wood in axial direction was one to two orders of magnitude faster than in the radial direction.

Effect of gas permeation

The results indicate that estimated permeation values of the skin and cortex tissue in the radial direction were not

significantly different while the permeation of tissue along the vertical axis was much higher compared with the permeation in the cortex tissue in the radial direction. The permeation coefficient for the gas along the vertical axis was high compared to the radial direction (Table 1). The bulk gas transport along the vertical axis is probably facilitated by means of better continuity of the gas filled spaces.

The permeation coefficient of the tissue may contribute to gas transport besides diffusion; the CO_2 diffusivity of the tissue was higher than the O_2 diffusivity (Marcellin, 1974; Lammertyn *et al*., 2001; Schotsmans *et al*., 2003, 2004; Ho *et al*., 2006*a*). The produced CO_2, therefore, leaves the fruit at higher rates than O_2 is entering the fruit. This may lead to a pressure difference between the inside of the fruit and the external atmosphere. A pressure rise was found in the measurement chamber in diffusion measurement for specific initial gas conditions (Ho *et al*., 2006*a*). In gas transport experiments with a mixture of gases, for example gas diffusion in fruit, the total pressure changes should be considered carefully, and if significant, permeation should be included. Because the O_2 consumption rate and CO_2 production rate were not the same in pear, permeation plays an important role in balancing the total pressure inside the fruit to the external environment.

Conclusion

A measurement set-up for gas permeation in fruit tissue based on unsteady-state gas exchange was developed. An analytical model described the experimental estimated permeation well. Permeation coefficients of the skin and tissue along the radial direction were more or less equal while permeability in the vertical axis was higher than along the radial direction. The permeation–diffusion–reaction model can be applied to study the gas transport in whole intact fruit.

While the model validation results were reasonably well correlated, a discrepancy between measured gas concentrations and model predictions remains. We believe that this is mainly due to the fact that, contrary to typical engineering materials such as steel or brick, biological tissue cannot be considered as a continuum material because of its cellular nature. A continuum model such as the one proposed in this article should, therefore, be considered as phenomenological and the transport properties as apparent properties. Multiscale transport models are currently being developed by the authors to quantify the cellular and intercellular pathways for gas transport and to improve agreement further between measured and predicted gas concentrations at the expense of much more computer resources.

Acknowledgements

The authors wish to thank the research council of the KU Leuven (project IDO/00/008, OT 04/31) for financial support. Acknowledgement is extended to the International Relations Office of the KU Leuven (IRO Scholarship). Pieter Verboven is postdoctoral researcher of the Flemish fund for Scientific Research (FWO-Vlaanderen).

References

Banks NH. 1985. Estimating skin resistance to gas diffusion in apples and potatoes. *Journal of Experimental Botany* **36,** 1842–1850.

Banks NH, Kays SJ. 1988. Measuring internal gases and lenticel resistance to gas diffusion in potato tubers. *Journal of the American Society of Horticultural Science* **113,** 577–580.

Bird RB, Stewart RB, Lightfoot EN. 2002. *Transport phenomena*. New York: John Wiley & Sons.

Burg SP, Burg EA. 1965. Gas exchange in fruits. *Plant Physiology* **18,** 870–874.

Cameron AC, Yang SF. 1982. A simple method for the determination of resistance to gas diffusion in plant organs. *Plant Physiology* **70,** 21–23.

Geankoplis CJ. 1993. *Transport processes and unit operations*. Englewood Cliffs, New Jersey: Prentice-Hall Inc.

Ho QT, Verlinden BE, Verboven P, Vandewalle S, Nicolaï BM. 2006*a*. Simultaneous measurement of oxygen and carbon dioxide diffusivities in pear fruit tissue using optical sensors. *Journal of the Science of Food and Agriculture* (in press).

Ho QT, Verlinden BE, Verboven P, Nicolaï BM. 2006*b*. Gas diffusion properties at different positions in the pear. *Postharvest Biology and Technology* **41,** 113–120.

Kader AA. 1988. Respiration and gas exchange of vegetables. In: Weichmann J, ed. *Postharvest physiology of vegetables*. New York: Marcel Dekker Inc., 25–43.

Lammertyn J, Scheerlinck N, Jancsók P, Verlinden BE, Nicolaï BM. 2003*a*. A respiration–diffusion model for 'Conference' pears. I. Model development and validation. *Postharvest Biology and Technology* **30,** 29–42.

Lammertyn J, Scheerlinck N, Jancsók P, Verlinden BE, Nicolaï BM. 2003*b*. A respiration–diffusion model for 'Conference' pears. II. Simulation and relation to core breakdown. *Postharvest Biology and Technology* **30,** 43–55.

Lammertyn J, Scheerlinck N, Verlinden BE, Schotsmans W, Nicolaï BM. 2001. Simultaneous determination of oxygen diffusivity and respiration in pear skin and tissue. *Postharvest Biology and Technology* **23,** 93–104.

Lide DR. 1999. *Handbook of chemistry and physics*. New York: CRC Press.

Mannapperuma JD, Sing RP, Montero ME. 1991. Simultaneous gas diffusion and chemical reaction in foods stored in modified atmospheres. *Journal of Food Engineering* **14,** 167–183.

Marcellin P. 1974. Conservation des fruits et legumes en atmosphere controllee, a l'aide de membranes de polymers. *Revue Generale du Froid* **3,** 217–236.

Nobel PS. 1991. *Physicochemical and environmental plant physiology*. London: Academic Press Inc., 1–46.

Quintard M, Bletzacker L, Chenu D, Whitaker S. 2006. Nonlinear, multicomponent, mass transport in porous media. *Chemical Engineering Science* **61,** 2643–2669.

Rajapakse NC, Banks NH, Hewett EW, Cleland DJ. 1990. Development of oxygen concentration gradients in flesh tissues of bulky plant organs. *Journal of the American Society for Horticultural Science* **115,** 793–797.

Schotsmans W, Verlinden BE, Lammertyn J, Nicolaï BM. 2004. The relationship between gas transport properties and the histology of apple. *Journal of the Science of Food and Agriculture* **84,** 1131–1140.

Schotsmans W, Verlinden BE, Lammertyn J, Nicolaï BM. 2003. Simultaneous measurement of oxygen and carbon dioxide diffusivity in pear fruit tissue. *Postharvest Biology and Technology* **29,** 155–166.

Sorz J, Hietz P. 2006. Gas diffusion through wood: implications for oxygen supply. *Trees–Structure and Function* **20,** 34–41.

Talasila PC, Cameron AC. 1997. Free-volume changes in flexible, hermetic packages containing respiring produce. *Journal of Food Science* **62,** 659–664.

Wood BD, Quintard M, Whitaker S. 2002. Calculation of effective diffusivities for biofilms and tissues. *Biotechnology and Bioengineering* **77,** 495–516.

Wood BD, Whitaker S. 1998. Diffusion and reaction in biofilms. *Chemical Engineering Science* **53,** 397–425.

Zhang J, Bunn JM. 2000. Oxygen diffusivities of apple flesh and skin. *Transactions of the ASAE* **43,** 359–363.